



CHORUS

This is the accepted manuscript made available via CHORUS. The article has been published as:

## Ionization of Na Rydberg atoms by a 79-GHz microwave field

A. Arakelyan, J. Nunkaew, and T. F. Gallagher

Phys. Rev. A **94**, 053416 — Published 17 November 2016

DOI: [10.1103/PhysRevA.94.053416](https://doi.org/10.1103/PhysRevA.94.053416)

# Ionization of Na Rydberg atoms by a 79 GHz microwave field

A. Arakelyan,<sup>1,\*</sup> J. Nunkaew,<sup>2</sup> and T. F. Gallagher<sup>1</sup>

<sup>1</sup>*Department of Physics, University of Virginia,  
Charlottesville, Virginia 22904-0714, USA*

<sup>2</sup>*Department of Physics and Materials Science, Faculty of Science,  
Chiang Mai University, Chiang Mai 50200, Thailand*

## Abstract

We have measured the ionization fields for Na Rydberg states of  $n \geq 26$  by a 79 GHz microwave field. At low  $n$ , where the microwave frequency  $\omega$  is one third the classical Kepler frequency  $\omega_K$ , which is equal to the  $1/n^3$  spacing between  $n$  states, the ionization field is  $\approx 1/3n^5$ , in atomic units. As  $n$  is raised  $\omega_K$  decreases, and the ionization field rises above  $1/3n^5$ , reaching a constant value when  $\omega = \omega_K$ . At very high  $n$ , where  $\omega > 1/2n^2$ , single photoionization is possible, and the measured rate agrees with the calculated value. These measurements, together with those done previously, connect the processes of field ionization and photoionization in Na. At low  $n$  and radio frequencies ionization is simply field ionization, and at very high  $n$  it occurs by photoionization, single photon absorption. These measurements also show that microwave ionization of Rydberg atoms at 79 GHz results in significant population's being left in the very high-lying states.

---

\* Current address: Department of Physics, University of Michigan, Ann Arbor, Michigan 48109, USA

## I. INTRODUCTION

To photoionize an atom a photon's energy must exceed the atom's binding energy, while to field ionize an atom the field must be large enough to depress sufficiently the coulomb potential on one side of the atom. There is a frequency criterion for photoionization (PI) and a field criterion for field ionization (FI). Multiphoton ionization (MPI) connects these two extreme cases, and the requirements for MPI involve both frequency and field.

While it is straightforward to ionize ground state atoms with intense laser fields, it is not possible to produce controlled static fields of the strength required for ionization, so the prospects for connecting FI to PI using ground state atoms are not bright. The obvious alternative is to use the excited states, in particular Rydberg states, those of high principal quantum number  $n$ . Since the binding energies of Rydberg states are small,  $\approx -1/2n^2$ , multiphoton ionization requires microwaves, not visible light. Unless noted otherwise, we use atomic units. The use of Rydberg atoms and microwaves to connect FI to PI by microwave ionization (MWI) was pioneered by Bayfield and Koch, who explored microwave ionization of Rydberg states of H [1].

It is reasonable to expect the classical Kepler orbital frequency  $\omega_K = 1/n^3$ , the frequency for the hydrogenic  $n \rightarrow n + 1$  transition, to define an approximate boundary between FI and PI. If the microwave frequency  $\omega$  is less than  $\omega_K$  ionization is more likely to resemble FI, but if  $\omega > \omega_K$  it is more likely to resemble PI. In H, at least in the  $\omega < \omega_K$  regime, this expectation is met [1, 2]. However, in any other atom it is not, because the Rydberg electron does not experience a pure  $-1/r$  Coulomb potential, rather, one which is deeper at small  $r$  due to the finite sized ionic core. Here  $r$  is the distance of the Rydberg electron from the center of the ion. In spite of the fact that FI and MWI are very different in H and other atoms, it is possible in both cases to connect FI to PI, and here we describe the completion of this connection for Na. Specifically, we describe MWI experiments using a 79 GHz microwave field to ionize Na atoms, from low  $n$  states,  $n \approx 25$ , for which  $\omega \approx \omega_K/3$  to very high  $n$  states for which  $\omega > 1/2n^2$ . At low  $n$  an ionization field  $E \approx 1/3n^5$  is observed, as seen previously [3, 4], and at high  $n$  single photon ionization occurs [5].

This paper is organized in the following way. To provide perspective for the present work we first describe the FI to PI connections in H and Na, which are very different. We then outline the experimental approach and present our results for 79 GHz ionization of Na and

the conclusions which can be drawn from them.

## II. FROM FIELD IONIZATION TO PHOTOIONIZATION

### A. Hydrogen

Field ionization and microwave ionization in hydrogen for  $\omega \ll \omega_K$  can both be understood by examining the energy level diagram of Fig. 1, in which we show the energy levels of  $m = 0$  levels of  $19 \leq n \leq 20$  as a function of electric field [6–8]. Here  $m$  is the electron’s angular momentum in the field ( $z$ ) direction. As shown, the levels exhibit very nearly linear Stark energy shifts. In the presence of a field, the zero field  $\ell$  states are converted to Stark states which have permanent electric dipole moments. Here  $\ell$  is the electron’s total orbital angular momentum, which is not a good quantum number in the presence of a field, although  $m$  is. In the blue states, those shifted up in energy, the Rydberg electron is found predominately on the uphill side of the atom-field potential, and in the red states, those shifted down in energy, the electron is found on the downhill side of the potential. The two extreme  $|m| = 0$  states exhibit shifts given by [6]

$$\Delta_{r,b} = \pm \frac{3n^2 E}{2}, \quad (1)$$

and the extreme blue and red states of  $n$  and  $n + 1$  cross at the Inglis-Teller field  $E = 1/3n^5$ . The lines showing the levels end at the fields at which the FI rate is  $10^6 \text{ s}^{-1}$ . The lower energy, red, states ionize at lower static fields than the blue states since in the red states the Rydberg electron is close to the saddle point in the potential, while in the blue states the electron is held away from the saddle point by something analogous to a centrifugal potential. The reddest states ionize at the classical limit for ionization shown by the broken line in Fig. 1. In the potential

$$V = -\frac{1}{r} - Ez, \quad (2)$$

the saddle point occurs at the energy  $W_S$ . Measured relative to the zero field ionization limit  $W_S$  is given by

$$W_S = -2\sqrt{E}. \quad (3)$$

Stated differently, the field required for ionization is

$$E = \frac{W_S^2}{4}, \quad (4)$$

which, if we ignore Stark shifts, is often written as

$$E = \frac{1}{16n^4}. \quad (5)$$

As shown by Fig. 1 and Eq. (1) the reddest Stark state exhibits a shift of  $-3n^2E/2$  to lower energy, and, when this shift is taken into account, we find that the reddest Stark state ionizes at the field [4, 8]

$$E = \frac{1}{9n^4}. \quad (6)$$

An important aspect of Fig. 1 is that the blue states of  $n = 20$  are not coupled to the red states of  $n = 21$ ; the electron is on opposite sides of the atom in these two states. At fields below the classical ionization limit, blue and red states cross each other (if we ignore the electron's spin), and, above the classical limit, the blue states are stable, in spite of their degeneracy with rapidly ionizing red states of higher  $n$ . The blue states of  $n = 20$  are, however, coupled to the blue states of  $n \neq 20$ , and these couplings lead to a second order Stark shift of the levels, to lower energy. As a result of these couplings, the Stark shifts are not perfectly linear, although the deviation from linearity is not visible in Fig. 1.

If a hydrogen atom is excited in zero field and then exposed to a ramped ionization field, it is first projected, at very low field, onto the Stark states. Once in a Stark state the atom remains in the same state as the field is raised to the field at which ionization occurs. All the level crossings of Fig. 1 are traversed diabatically.

For  $\omega \ll \omega_K$  microwave ionization occurs at the field  $E = 1/9n^4$ , the static field required for ionization of the reddest Stark state. The same  $\Delta n \geq 1$  blue to blue and red to red couplings, which lead to the second order Stark shift in a DC field, couple the red and blue states of the same  $n$  by a Raman coupling, and all  $|m| = 0$  atoms of the same  $n$  ionize via the reddest state at the field  $E = 1/9n^4$ . As the microwave frequency is raised, so that  $\omega$

approaches  $\omega_K$ , the microwave field required for ionization decreases, and clear multiphoton  $\Delta n = 3$  and  $\Delta n = 2$  resonances are observed when  $\omega = \omega_K/3$  and  $\omega_K/2$  [1, 2]. These two phenomena indicate that in this frequency regime ionization occurs by making transitions to higher lying states followed by ionization.

Although systematic ionization measurements in the  $\omega > \omega_K$  regime have not been carried out for H, for  $\omega > \omega_K$ , the high  $n$  regime, a one dimensional model predicts ionization to occur by a sequence of transitions through progressively higher lying states, with the required field for ionization given by [9, 10]

$$E = \frac{2.4}{\omega^{5/3}}, \quad (7)$$

which is independent of  $n$ . The  $n$  independence arises in the following way. The  $n \rightarrow n'$  Rabi frequency  $\Omega_{n,n'}$  is given in the rotating wave approximation by [9, 10]

$$\Omega_{n,n'} = \langle n|z|n'\rangle E/2 = \frac{0.41E}{2(nn')^{3/2}\omega^{5/3}}, \quad (8)$$

which is equated to the maximum detuning  $\delta_{n,n'} = 1/2n^3$  of the microwave frequency from the  $n \rightarrow n'$  resonance frequency. This expression for the matrix element is only valid if  $|n - n'| > 1$ . In the high  $n$  regime of interest  $n \approx n' \gg 1$ , and equating the Rabi frequency to the maximum detuning leads immediately to the threshold field of Eq. (7). This model breaks down when the initial state is only a few photons from the limit, where ionization is better characterized by a rate. Finally when  $\omega > 1/2n^2$  single photon ionization occurs, with a readily calculable rate [5].

## B. Sodium

While the field ionization of hydrogen has long been understood, the same cannot be said for other atoms. It is more complex, due to the finite size of the ionic core. However, both FI and MWI in the  $\omega \ll \omega_K$  regime can be easily understood by examination of the energy level diagram of Fig. 2, the Na analog of Fig. 1, but for levels of  $|m| = 1$  [11]. We show  $|m| = 1$  levels in Fig. 2 because the  $m = 0$  avoided crossings are so badly overlapped that they are not recognizable as such. To show the details more clearly, the scale is expanded relative to the one used in Fig. 1.

While there are similarities to Fig. 1, there are two obvious differences, both due to the ionic core. First, the zero field  $np$  states are energetically removed from the higher  $\ell$  states. Second, there are now avoided crossings between the blue  $n = 20$  and red  $n = 21$  states and the red  $n = 20$  and blue  $n = 19$  states. In Fig. 2 the shaded region is above the classical ionization limit, and in this region all states ionize on time scales of  $10^{-7}$  to  $10^{-10}$  s. While in H the blue states require much higher fields than the red states for ionization, in Na this is not the case. In Na the ion core couples blue and red states of different  $n$ . At fields below the classical limit, this coupling lends to the obvious avoided crossings of Fig. 2. The avoided crossings exhibit a  $1/n^4$  scaling and depend on  $m$ . Above the classical limit, the coupling of blue states to ionizing red states of higher  $n$  results in ionization. As shown by Littman *et al.* [12], these red states do not comprise a true continuum, but the practical effect is the same [12].

The presence of the avoided crossings in Fig. 2 introduces an additional frequency scale into the problem, the typical size  $\Omega$  of the avoided crossing. When Na atoms are excited to low  $\ell$  states in zero field and exposed to a ramped field with a  $1\text{-}\mu\text{s}$  risetime, they pass adiabatically from zero field to the high ionizing field and ionize at the classical ionization limit  $E = 1/16n^4$ . As shown by Fig. 2, the adiabatic paths from the zero field  $n = 20$  states are trapped between those from  $n = 19$  and  $n = 21$ . Unlike H, in fields above the Inglis-Teller field the atoms gain essentially no energy. At a frequency of 10 MHz the avoided crossings of Fig. 2 are also traversed adiabatically, and ionization occurs at the classical ionization field, the same field at which pulsed field ionization occurs [8, 13]. In an oscillating field the avoided crossings of the high  $\ell$  states at zero field are traversed diabatically, but  $n$  is unchanged [14]. Since the  $n = 20$  states are trapped between the  $n = 19$  and  $n = 21$  states, ionization can only occur over a small range of fields around  $E = 1/16n^4$ .

At a frequency of 670 MHz Na atoms no longer traverse the avoided crossings of Fig. 2 adiabatically. As a result, atoms initially excited to the  $n$  state and exposed to a 670 MHz field exceeding  $E = 1/3n^5$  pass through the first avoided crossing at the Inglis-Teller field twice and can undergo Landau-Zener transitions to the  $n + 1$  state. By similar  $n \rightarrow n + 1$  transitions the atoms continue to gain energy until they are ionized by the field. As a result, at 670 MHz the threshold field for ionization is slightly higher, 20%, than  $E = 1/3n^5$ . As the frequency of the field is raised into the microwave regime, the threshold field slowly decreases, and at 15 GHz the ionization field is 15% below  $E = 1/3n^5$ , which is not consistent with the

single cycle Landau-Zener picture given above [4, 13, 15]. The ionization below  $E = 1/3n^5$  is a result of the coherent addition of  $n \rightarrow n + 1$  transition amplitudes from successive field cycles [16, 17].

In H as the ratio  $\omega/\omega_K$  is increased by raising  $n$ , transitions to higher lying states become progressively more important, and the ionization field for fixed  $\omega$  falls progressively further below  $E = 1/9n^4$  [2]. In Na, as  $n$  is increased, the ionization fields increase above  $E = 1/3n^5$  since the avoided crossings and core couplings become smaller [13, 18]. The resonances seen in H when  $\omega = \omega_K/3$  and  $\omega = \omega_K/2$  are not visible in Na, due to its ionic core, although they are in Li, which has a very small core [19].

When  $\omega = \omega_K$ , the ionization fields for H and Na are calculated to be identical [18], and for  $\omega > \omega_K$  the 79 GHz experiments we report here confirm that the theoretical description of ionization of H given earlier also describes ionization of Na [9, 10], as predicted theoretically [18]. In particular, the ionization field for a fixed frequency is independent of  $n$  and given by Eq. (7) to within a few microwave photons of the limit, where a photoionization rate provides a better description [5].

### III. EXPERIMENTAL APPROACH

A thermal beam of ground state sodium atoms crosses the microwave electric field antinode at the center of a 79.05-GHz Fabry-Perot microwave cavity. These atoms are excited to a Rydberg state by the sequence of transitions  $3s \rightarrow 3p \rightarrow 3d \rightarrow nf$  induced by three 20-ns laser pulses, at wavelengths of 589, 818, and 826-814 nm, as shown in the timing diagram of Fig. 3. After laser excitation, atoms are subjected to a microwave pulse, typically 500-ns long. About 300 ns after the end of the pulse, atoms are exposed to a 1- $\mu$ s rise time field ionization pulse (FIP). Depending on the polarity of the FIP, either electrons or ions are driven upward to a dual microchannel plate (MCP) detector. The MCP signal is amplified, captured by a gated integrator or oscilloscope, and recorded in a computer for later analysis.

The Fabry-Perot microwave cavity consists of two brass mirrors 69.7 mm in diameter with 52-mm radii of curvature. The on-axis spacing between mirrors is 90.51 mm. The cavity is operated on the TEM<sub>048</sub> mode at a frequency of 79.05 GHz with  $Q = 8600$ . The microwave system generates a 79.05-GHz pulse with 0 to 180 V/cm amplitude and a variable width. The microwave field amplitude is calibrated using the method described by Cheng *et al.*

[20], and we are able to determine the amplitude of the microwave field with an uncertainty of 15%.

The experiment is triggered at the 1-kHz repetition rate of the frequency-doubled Nd:YLF laser used to pump the dye lasers. The first 527-nm pulse pumps a  $3s - 3p$  Littman-Metcalf dye laser. The second pump beam is used for a near infrared Littman-Metcalf dye laser that drives the last transition [21]. The linewidth of this laser is about 10 GHz. Amplified spontaneous emission of the second laser drives the  $3p - 3d$  transition, while the coherent output of the oscillator populates an  $nf$  Rydberg state. Although the spontaneous emission can effectively drive the  $3p - 3d$  transition, it is not strong enough to excite an observable number of atoms to Rydberg states or to photoionize them. To populate the  $3d$  level more efficiently, we have also used a Toptica DL100 infrared diode laser to drive the  $3p - 3d$  transition. To avoid undesirable photoionization of atoms by the 589-nm laser, the output of the diode laser is sent through a Pockels cell that is triggered in such a way that the cw beam is off during the first step of the excitation process. The laser beams are sent to the vacuum chamber, pass through 1-cm holes in the bias voltage plates on either side of the cavity, and are focused to less than 1-mm diameter spots where they cross the atomic beam. In addition to the bias plates on the sides of the cavity, bias voltages are also applied to the top and bottom plates and the cavity mirrors to reduce the stray static field to 2 mV/cm. Unless stated otherwise, the laser field and microwave field are polarized vertically.

#### IV. EXPERIMENTAL OBSERVATIONS

We have measured the 10% and 50% ionization fields for 500-ns 79-GHz pulses. At fixed tunings of the laser, we observe the atoms which survive the 500-ns 79-GHz pulses of variable amplitude, and in Fig. 4 we show the electron signal resulting from field ionization of atoms which have survived the microwave pulse vs. the microwave field amplitude. As shown in Fig. 4, even at the highest microwave fields, roughly 10% of the atoms remain bound. As discussed elsewhere in some detail, these atoms are left in the extremely high-lying states,  $n > 250$ , in which the Rydberg electron infrequently returns to the ion core where it can absorb energy from the microwave field [22]. In Fig. 5 we plot the fields at which 90% and 50% of the atoms survive the pulse, or 10% and 50% of the atoms are ionized. An obvious feature of Fig. 5 is the non monotonic variation of threshold fields

with  $n$  or binding energy, which arises from multiphoton resonances. For example, at 79.05 GHz  $n = 29$  and  $36$  do not have multiphoton resonances with higher lying states, while the neighboring states do, resulting in the higher ionization fields for  $n = 29$  and  $36$ . These two states, at energies of  $-3920$  and  $-2538$ , GHz are marked by arrows in Fig. 5. The non-monotonic  $n$  dependence of the ionization fields seen in Fig. 5 was not observed at much lower microwave frequencies [3, 15]. The effect of resonance on the ionization fields is hardly unexpected since the production of high-lying states exhibits clearly resonant behavior [22]. A second difference from microwave ionization at much lower frequencies is a dependence of the ionization fields on microwave pulse length. At 8 and 15 GHz the ionization fields were pulse length independent for pulse more than 200 ns long [4, 15]. At 79 GHz, lengthening the pulse from 500 ns to 1  $\mu$ s results in a 20% decrease in the ionization field.

The dot-dashed and dotted lines of Fig. 5 indicate the fields  $E = 1/3n^5$  and  $1/9n^4$ , respectively. For  $n = 26$ , the lowest energy state shown in Fig. 5,  $\omega/\omega_K \approx 1/3$ , so we are never in the  $\omega \ll \omega_K$  limit where the 50% ionization field is slightly below  $E = 1/3n^5$  (at the same  $n$  a frequency of 15 GHz leads to  $\omega/\omega_K = 1/16$ ). However, the 10% ionization fields do occur slightly below  $E = 1/3n^5$  for the lowest  $n$  states of Fig. 5, but, as the energy is raised above  $-3500$  GHz, the 10% ionization fields evolve toward  $E = 1/9n^4$ . As shown, only for  $n \geq 30$  we are able to observe more than 50% ionization, and at  $n = 30$  the 50% ionization field is closer to  $E = 1/3n^5$  than to  $E = 1/9n^4$ , and as  $n$  is increased the ionization field evolves to  $E = 1/9n^4$ . From the binding energy  $-1400$  GHz,  $n = 48$ , to the energy  $-800$  GHz,  $n = 64$ , the ionization fields are  $n$ , or energy, independent. In this region the ionization fields are approximately 30% lower than the dotted line of Fig. 5 (b), which is the prediction of Eq. (7) for  $\omega > \omega_k$ .

At energies above  $-800$  GHz, the threshold fields on average decrease toward zero, and they exhibit oscillatory structure at the microwave frequency of 79 GHz. The origin of the oscillatory structure is that states which are in multiphoton resonance with high-lying states just below the ionization limit are driven to the high-lying states in which the Rydberg electron does not often return to the ion core where it can absorb another microwave photon and ionize.

Near the limit microwave ionization is better characterized by a rate than a threshold field. Accordingly, we have measured the photoionization rates with the laser tuned 0.5, 1.0, 1.5, and 2 MW photons below the zero field ionization limit. The atoms were exposed

to microwave pulses of fixed amplitude, from 1 to 4.6 V/cm, and variable length, and the number of surviving atoms detected as a function of pulse length. We observed a rapid initial decay in the number of atoms detected and a long tail, as exemplified by Fig. 6. We fit the observed decays to the sum of an exponential and a constant, and we identify the initial fast decay rate as the photoionization rate of the initially populated state, which results in the rates shown in Fig. 7.

As shown by Fig. 7, the fastest rates are observed for the laser tuned one MW photon below the limit so that the absorption of one MW photon produces a free, near zero energy electron. With a laser tuning of 0.5 MW photon below the limit absorption of one MW photon also leads to photoionization, but at a much reduced rate. Both of these observed rates can be compared to the single photon ionization rates calculated using the matrix elements of Delone *et al.* [23]. Specifically, the photoionization rate  $\Gamma$  of an initial state of principal quantum number  $n_i$  to the continuum  $f$  produced by the microwave field  $E\cos\omega t$  is given by

$$\Gamma = 2\pi|\langle n_i|z|f\rangle E/2|^2, \quad (9)$$

where we have used the rotating wave approximation ( $E/2$ ), the radial matrix element

$$\langle n_i|r|f\rangle = \frac{0.41}{n^{3/2}\omega^{5/3}}, \quad (10)$$

and the  $m = 0$  angular  $nf \rightarrow \epsilon g$  matrix element. In Eqs. (9) and (10) the continuum  $|f\rangle$  is normalized per unit energy. The resulting photoionization rate exhibits a  $1/n^3$  scaling, i. e.  $\Gamma \propto 1/n^3$ , which is why the photoionization rate for the laser tuning 0.5 MW photons below the limit is smaller than the rate for the tuning of 1 MW photon below the limit. The calculated photoionization rates for laser tunings 0.5 and 1.0 MW photons below the limit are shown by the broken and solid lines, respectively, in Fig. 7. At low fields they are both in good agreement with the observed rates and exhibit the expected  $1/n^3$  variation. However, at higher fields the data for the tuning 0.5 MW photons below the limit fall well below the calculation. What may be surprising is that the rates for two photon ionization, observed with the laser tuning of 2 MW photons below the limit, are higher than the single photon rate for a tuning of 0.5 MW photon below the limit. This difference is due to the fact that with a tuning of 0.5 MW photons below the limit laser excitation puts atoms in states in which the the electron rarely returns to the core. In contrast, with a laser tuning

of two MW photons below the limit ionization can occur by a transition to a state bound by one MW photon followed by rapid single photon ionization.

The time resolved field ionization signals show that for laser tunings of 2, 3, and 4 photons below the limit the atoms pass through real intermediate states en route to ionization, as shown by oscilloscope traces of time resolved field ionization signals. In Fig. 8 we show, for reference, the oscilloscope traces obtained with the laser tuned 1, 2, 3, and 4 photons below the limit with no microwave pulse. The figure also contains the trace obtained with the laser tuned four photons below the limit after exposure to a 30-ns 60-V/cm microwave pulse. Subsequent to the microwave pulse, population is found in the states 1, 2, and 3 photons below the limit, as it moves through these states en route to ionization.

Laser excitation with tunings of half integral numbers of MW photons below the limit results in very different field ionization signals due to atoms' being trapped in high lying states  $\approx 0.5$  MW photons below the limit. In Fig. 9 we show, for reference, the traces obtained with the laser tuned 0.5 or 3.5 MW photons below the limit without the microwave pulse. When the laser is tuned 3.5 photons below the limit and a microwave pulse of 30 or 60 V/cm is present, the large signal from the states 0.5 MW photons below the limit obscures whether or not there are atoms left in intermediate states 1.5 and 2.5 MW photons below the limit. The dominant effect is the trapping of substantial population 0.5 MW photons below the limit. The difference between the oscilloscope traces of Figs. 8 and 9 is simply another manifestation of the oscillation in the ionization field shown in Fig. 5 (b).

It is useful to return to the long tail of Fig. 6, which reflects an enormous reduction in the photoionization rate at later times. We attribute the tail to the conversion of the  $\ell = 3$  states initially excited by the laser into high  $\ell$  and  $|m|$  states, which have much smaller photoionization cross sections, since in these states the electron never comes close to the  $\text{Na}^+$  core. In Fig. 10, we show the calculated squared radial photoionization matrix elements  $|\langle 60\ell|r|\epsilon\ell + 1\rangle|^2$  for H  $n = 60$  states as a function of  $\ell$  for several photon frequencies. We have used  $n = 60$  for numerical reasons, but the conclusions drawn from the calculations are not dependent on  $n$ . A frequency of 914 GHz brings an  $n = 60$  atom to the limit, while 1314 and 1634 GHz frequencies take the atom well above the limit. The photoionization rate is proportional to the product of the squared radial and angular matrix elements. Since the linearly polarized microwave field defines the quantization axis, the relevant squared angular matrix element for photoionization is

$$|\langle \ell m | \hat{z} | \ell + 1 m \rangle|^2 = \frac{(\ell + 1)^2 - m^2}{(2\ell + 3)(2\ell + 1)}, \quad (11)$$

which is of order unity for small  $|m|$  and goes to zero as  $|m|$  approaches  $\ell$ . If  $|m|$  remains small so that only averaging over  $\ell$  occurs, the variation in the photoionization rate is only due to the radial variation shown in Fig. 10, which results in an average rate approximately equal to the low  $\ell$  rate, which is not consistent with what we observe. For this reason we believe that population moves into higher  $|m|$  states, which reduces the average photoionization rate for two reasons. First, the high multiplicity of the high  $\ell$  states combined with the small radial matrix elements reduces the average rate. Second, even for states of  $\ell < n/2$  the angular matrix element goes to zero as  $|m| \rightarrow \ell$ .

It is not so surprising that atoms are driven to states of higher  $\ell$ . One mechanism is microwave driven Raman transitions through lower lying states and the continuum. Raman transitions driven by the microwave field do not, however, change  $m$ . Changing  $m$  requires a perpendicular magnetic or electric field, and we have both. The residual stray electric field in the horizontal plane is approximately 5 mV/cm, and the earth's magnetic field is not compensated, leading to a horizontal component of approximately 0.3 Gauss. Let us first consider the effect of a small stray electric field, ignoring for a moment the microwave field. The 20 ns laser pulse produces a wavepacket, which, due to the stray field  $E_S$ , oscillates between low and high  $\ell$  states at the frequency

$$\omega_{Stark} = 3nE_S, \quad (12)$$

the frequency spacing between the Stark levels of the same  $m$  and principal quantum number  $n$  in the stray field  $E_S$ . For  $n = 200$ , 80 GHz below the limit, and  $E_S = 5$  mV/cm,  $\omega_{Stark}/2\pi = 4$  MHz. Consequently, at times more than 125 ns after laser excitation high angular momentum states are present. Since the residual stray field is unlikely to be aligned with the microwave field, the evolution to high  $\ell$  but low  $|m|$  relative to the stray field corresponds to evolution to high  $|m|$  relative to the microwave field direction, suppressing the ionization rate. The importance of population transfer to higher  $|m|$  states has been shown by the observations of recombination by microwave fields and half cycle pulses perpendicular to static fields [24, 25]. It is also thought to be very important in zero kinetic energy (ZEKE) spectroscopy [26]. In ZEKE spectroscopy laser excitation of low  $\ell$ , molecular Rydberg states

with rapid predissociation rates results in long lived Rydberg states, due to collisional  $\ell$  and  $m$  mixing. In sum, it appears likely that small fields perpendicular to the microwave field play an important role in the survival of the high-lying states in the presence of a strong microwave field.

## V. CONCLUSION

Previous measurements at frequencies down to 10 MHz have shown the connection between field ionization and microwave ionization. These 79 GHz microwave ionization measurements connect microwave ionization to photoionization, completing the connection between field ionization and photoionization via multiphoton ionization.

## VI. ACKNOWLEDGEMENTS

This work has been supported by the National Science Foundation, through grant PHY-1206183, and by the U. S. Department of Energy, Basic Energy Sciences, Chemical Sciences Division, through grant DE-FG02-97ER14786. J. Nunkaew would like to thank DPST Research Grant No. 030/2557 for its support.

- 
- [1] J. E. Bayfield and P. M. Koch, Phys. Rev. Lett. **33**, 258 (1974).
  - [2] P. Koch and K. van Leeuwen, Phys. Rept. **255**, 289 (1995), ISSN 0370-1573.
  - [3] P. Pillet, R. Kachru, N. H. Tran, W. W. Smith, and T. F. Gallagher, Phys. Rev. Lett. **50**, 1763 (1983).
  - [4] P. Pillet, H. B. van Linden van den Heuvell, W. W. Smith, R. Kachru, N. H. Tran, and T. F. Gallagher, Phys. Rev. A **30**, 280 (1984).
  - [5] A. Schelle, D. Delande, and A. Buchleitner, Phys. Rev. Lett. **102**, 183001 (2009).
  - [6] H. A. Bethe and E. E. Salpeter, *Quantum mechanics of one- and two-electron atoms* (Dover, New York, NY, 2008).
  - [7] E. Luc-Koenig and A. Bachelier, J. Phys. B **13**, 1769 (1980).
  - [8] T. F. Gallagher, *Rydberg Atoms* (Cambridge University Press, 1994), ISBN 9780511524530, cambridge Books Online.

- [9] R. V. Jensen, S. M. Susskind, and M. M. Sanders, *Phys. Rev. Lett.* **62**, 1476 (1989).
- [10] R. Jensen, S. Susskind, and M. Sanders, *Phys. Rept.* **201**, 1 (1991), ISSN 0370-1573.
- [11] M. L. Zimmerman, M. G. Littman, M. M. Kash, and D. Kleppner, *Phys. Rev. A* **20**, 2251 (1979).
- [12] M. G. Littman, M. L. Zimmerman, and D. Kleppner, *Phys. Rev. Lett.* **37**, 486 (1976).
- [13] C. R. Mahon, J. L. Dexter, P. Pillet, and T. F. Gallagher, *Phys. Rev. A* **44**, 1859 (1991).
- [14] R. G. Rolfes, D. B. Smith, and K. B. MacAdam, *J. Phys. B* **16**, L533 (1983).
- [15] H. B. van Linden van den Heuvell and T. F. Gallagher, *Phys. Rev. A* **32**, 1495 (1985).
- [16] P. Pillet, C. H. Mahon, and T. F. Gallagher, *Phys. Rev. Lett.* **60**, 21 (1988).
- [17] R. C. Stoneman, D. S. Thomson, and T. F. Gallagher, *Phys. Rev. A* **37**, 1527 (1988).
- [18] A. Krug and A. Buchleitner, *Phys. Rev. Lett.* **86**, 3538 (2001).
- [19] M. W. Noel, W. M. Griffith, and T. F. Gallagher, *Phys. Rev. A* **62**, 063401 (2000).
- [20] C. H. Cheng, C. Y. Lee, and T. F. Gallagher, *Phys. Rev. A* **54**, 3303 (1996).
- [21] M. G. Littman and H. J. Metcalf, *Appl. Opt.* **17**, 2224 (1978).
- [22] A. Arakelyan and T. F. Gallagher, *Phys. Rev. A* **93**, 013411 (2016).
- [23] N. B. Delone, S. P. Goreslavsky, and V. P. Krainov, *J. Phys. B* **27**, 4403 (1994).
- [24] C. M. Evans, E. S. Shuman, and T. F. Gallagher, *Phys. Rev. A* **67**, 043410 (2003).
- [25] J. G. Zeibel and R. R. Jones, *Phys. Rev. Lett.* **89**, 093204 (2002).
- [26] W. A. Chupka, *J. Chem. Phys.* **98**, 4520 (1993).

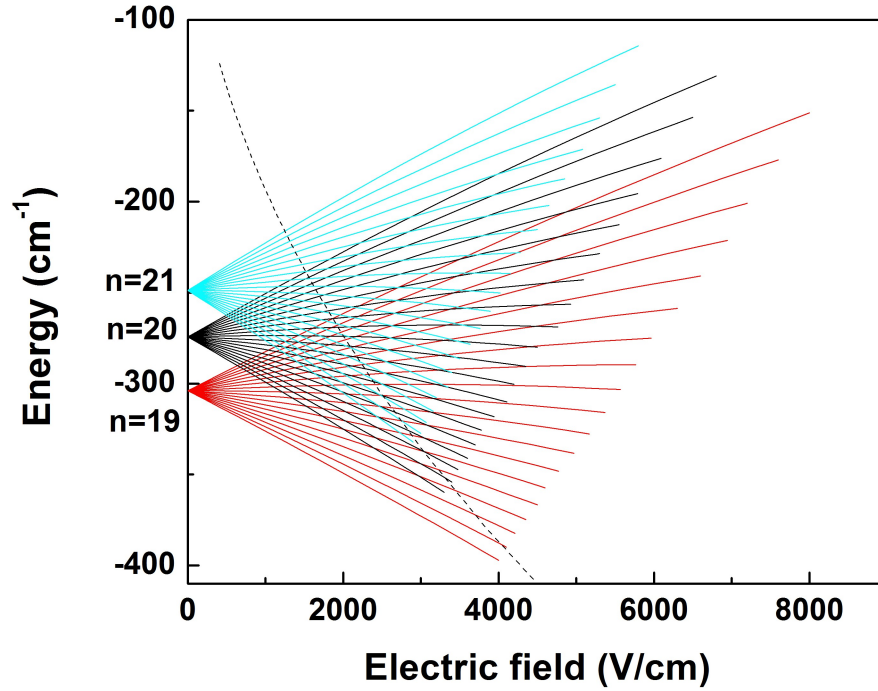


FIG. 1. Energy level diagram for H  $m = 0$  levels of  $19 \leq n \leq 21$  in electric fields of 0 to 8 kV/cm. The line for each level ends at the field at which the level's ionization rate is  $10^6 \text{ s}^{-1}$ . Note that the levels of different  $n$  cross, and that the blue shifted levels ionize at higher fields than do the red shifted levels. The red shifted levels ionize at the classical limit for ionization, indicated by the broken line.

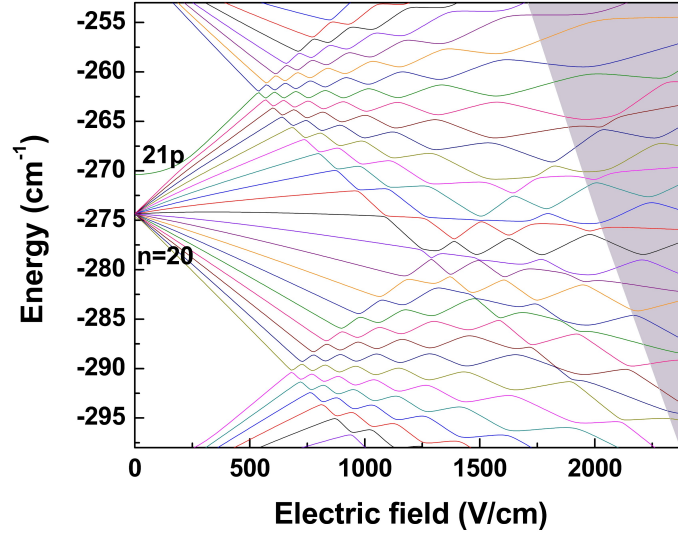


FIG. 2. Energy level diagram for Na  $|m| = 1$  levels of  $n = 20$  in electric fields of 0 to 2.4 kV/cm. The finite size of the  $\text{Na}^+$  core produces several differences from the H levels shown in Fig. 1. The zero field  $np$  energies are displaced from the hydrogenic energies, and there now avoided crossings between levels of different  $n$ . The region above the classical ionization limit is shaded, and in this region all levels have ionization rates in excess of  $10^6 \text{ s}^{-1}$ , but the levels are still relatively sharp, with ionization rates less than  $10^{10} \text{ s}^{-1}$ .

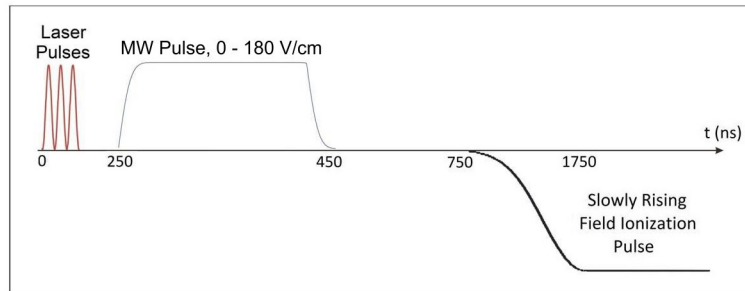


FIG. 3. Experimental timing diagram. Rydberg states created in laser excitation are subjected to the microwave pulse. About 300 ns after the microwave pulse, a slowly rising FIP ionizes atoms, and either electrons or ions are detected by the MCP, depending on the polarity of the FIP.

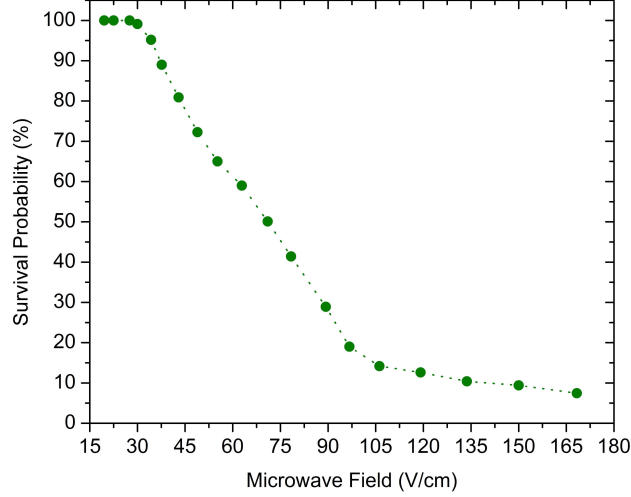


FIG. 4. Observed field ionization signal vs microwave field following excitation of the  $n = 55$  state. Unlike early microwave ionization experiments, ionization is not complete. Approximately 10% of the atoms are left in high-lying states, even with microwave fields as high as 170 V/cm.

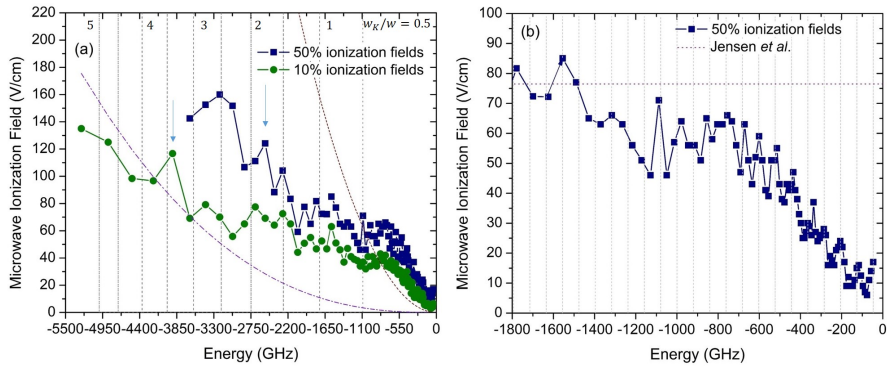


FIG. 5. (a) Microwave fields as a function of laser tuning for 50% and 10% ionization. Microwave pulse width is 500 ns. Vertical dashed lines on the graph correspond to the energies of Rydberg states for which the classical Kepler frequency equals  $5w - 0.5w$ . The dot-dashed and dotted lines indicate the fields  $E = 1/3n^5$  and  $1/9n^4$ , respectively. The arrows indicate  $n = 29$  and  $n = 36$ . (b) An expanded view of the 50% ionization fields in the  $w/w_K > 1$  regime. Up to  $-500$  GHz, our result is in agreement with a prediction of Jensen *et al.* [9] (red dotted line) that the average ionization field does not depend on  $n$ . That prediction, however, is not intended to reproduce the structure we observe. As shown by the vertical dashed lines spaced by  $w$ , the structure in the ionization fields is at the microwave frequency.

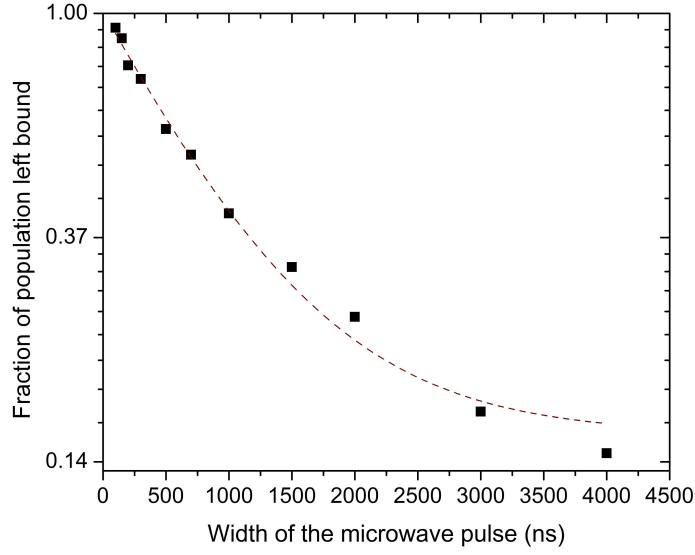


FIG. 6. Fraction of population left in bound states after the 1.8-V/cm microwave pulse of varied width. Atoms are excited to one microwave photon below the ionization limit (filled squares). Data points are fitted with an exponential decay curve of first order as  $Ae^{-t/\tau} + B$ .

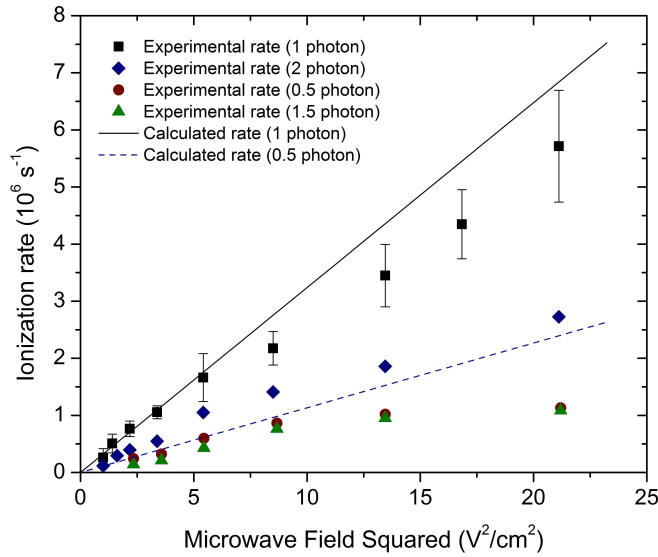


FIG. 7. Extracted single photoionization rates for several laser tunings below the ionization limit. The rates calculated using Fermi's Golden Rule, Eq. (9), for laser tunings of 0.5 and 1 photon below the limit are shown as broken and solid lines. The observed rates for the tuning of one photon below the limit are in a good agreement with the predicted values. For the tuning 0.5 photon below the limit the agreement is good only at low microwave fields.

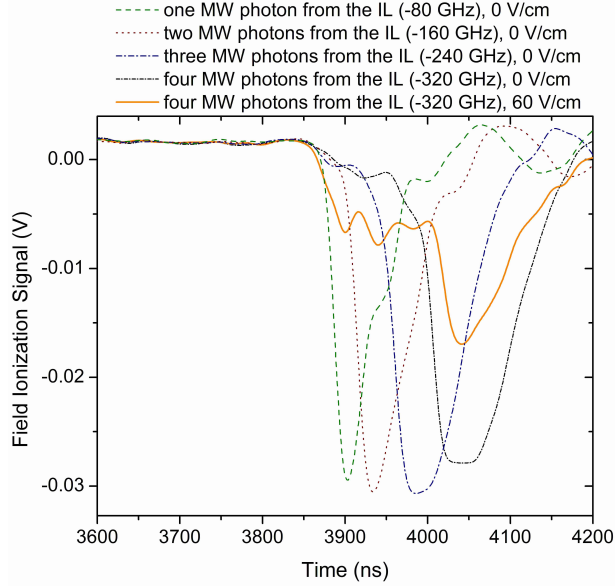


FIG. 8. An oscilloscope trace taken when the laser is tuned one, two, three, four MW photons from the IL with the microwave field off (broken lines), and when atoms are excited 4 MW photons from the IL and exposed to 60-V/cm 30-ns microwave pulse (solid line). The microwave field populates states three, two, and one photons below the IL where atoms photoionize.

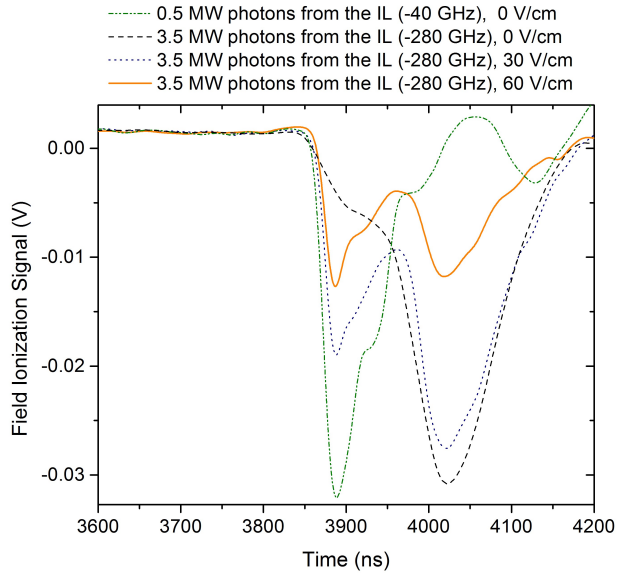


FIG. 9. An oscilloscope trace taken when the laser is tuned half a MW photon from the IL with the microwave field off (dash-dotted line) and 3.5 MW photons below it with the microwave field off (dashed line), after 30 V/cm 30-ns pulse (dotted line), and after 60 V/cm 30-ns pulse (solid line). The microwave field does not populate states between the initial state and states half a photon below the IL. Rather, a large fraction of population is found in the extremely high-lying states where atoms can survive long, large amplitude microwave pulses.

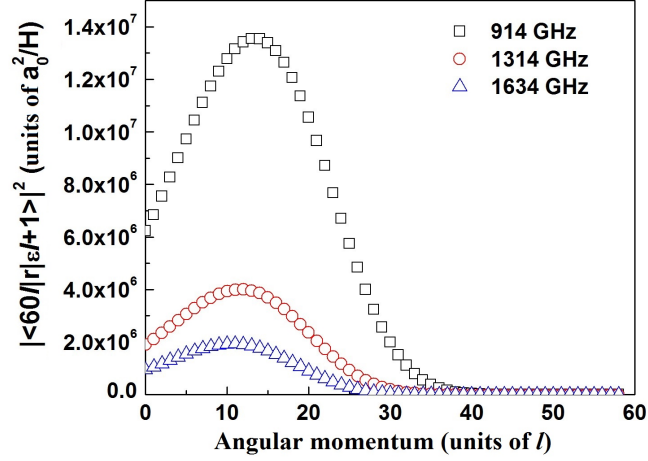


FIG. 10. Squared radial photoionization matrix elements for the H  $n = 60$  levels, in units of  $a_0^2/H$  (the squared Bohr radius/ Hartree), as a function of  $\ell$ . The binding energy of an  $n = 60$  level is 914 GHz. For all frequencies shown, the squared matrix element vanishes as  $\ell$  approaches 60, but the average squared matrix element is roughly equal to the low  $\ell$  value.